Effect of Nature Gas Injection on Reducibility of Wustite Prepared from Baharia Iron Ore Sinter

[1]M. Bahgat*, [2]K. S. Abdel Halim, [3]H. A. El-Kelesh, [4]M. I. Nasr

Central Metallurgical Research and Development Institute (CMRDI), P.O.Box 87-Helwan, Cairo, 11421, Egypt

[1]M_bahgat70@yahoo.com; *m_bahgat70@yahoo.com; [2]khsaad99@yahoo.com; [3]Heba_chemist2004@yahoo.com; [4]minasr@hotmail.com

***Abstract*-The main method for iron production is the blast furnace. It emits about 2 billion tons CO_2 per year, which has the largest contribution in global warming. Using thermo-gravimetric technique, wustite samples prepared from Baharia iron ore sinter were isothermally reduced at 900-1100 ^oC by different ratios of $H_2/CO/CO_2/N_2$ which is somewhat simulating the composition of the reducing gas in case of natural gas injection with low oxygen enrichment in the blast furnace. The reduction extent for wustite from iron ore sinter is clearly enhanced to be in the range of 54-69% comparatively with that reduced with coke gases (30-50%) as industrial data. Enhancement of wustite reducibility decreases the remaining quantity of unreduced wustite, which descends to high temperature region at which reduction depends mainly on solid carbon that will consequently lead to reduction of coke consumption and CO_2 emission. The reduction rate of wustite samples is independent on either the reaction temperature or the H_2 concentration in the reducing gas mixture due to the water gas shift reaction. The reduction rate of wustite samples at initial stages are most likely controlled by the combined effect of chemical reaction and gaseous diffusion mechanisms while at final stages are most likely controlled by interfacial chemical reaction mechanism.**

Keywords-Iron Making; Wustite; Natural Gas; Iron Ore; Sinter; CO_2 Emission

I. INTRODUCTION

Global climate change caused by green house gases has aroused wide concern in international society. According to International Panel on Climate Change (IPCC) report, there are four principle greenhouse gases result from human activities i.e. carbon dioxide, methane, nitrous oxide, and the halocarbons. Among these gases, CO_2 makes the largest contribution to global warning [1]. Since the iron and steel industry is energy intensive, CO_2 plays the most important role among these green house gases. The iron and steel industry is emitting about 650 million tons CO_2 per year as the fourth biggest industry using fossil fuels [2]. The amount of CO_2 emissions from iron and steel industry accounts for a great share of the total CO_2 emissions from industry [3]. Thus, reducing CO_2 emissions in iron and steel industry is urgent for environmental protection and sustainable development.

Some previous investigations handled the CO_2 emission reduction. Christer Ryman et al [4] studied reduction of CO_2 emissions from integrated steelmaking by optimized scrap strategies. An important aspect of the demonstrated calculations is that high scrap additions to an integrated system does not always act as a linear CO_2 diluent. It is important to optimize and balance the different processes in the considered system to ensure a global optimal solution.

Hisarna technology could reduce CO_2 emissions from blast furnace steelmaking by more than 50 percent [5]. The 20 million project is one of the initiatives that has sprung up under the auspices of ULCOS (ultra-low CO_2 steelmaking), a consortium of European steelmakers that has drawn up the world's most advanced program to reduce the steel industry's carbon footprint. The 60000 tpa Hisarna pilot plant will harness a new process that makes the production of liquid iron from virgin raw materials in just a single step possible, eliminating two of the three production steps required in blast furnace iron making. Hisarna opens the prospect of a 20% improvement in steel industry energy efficiency.

Also five blast furnace companies have joined together to reduce carbon dioxide (CO_2) emitted by the steel industry by 30% [6]. The greatest challenge is considered to be the development of technology for using hydrogen for the reduction of iron ore, or put more simply, technology for using hydrogen as the reduction agent to reduce the amount of coke inserted into the blast furnace. The oxygen enrichment has an insignificant effect on the performance indices [7]. The injection of natural gas reduces CO_2 emission but increases the energy consumption as compared to traditional iron making. The injection of geologically older solid natural fuels, e.g. high-, med-, or low volatile coals, reduces CO_2 emission, with simultaneous reduction of energy consumption indices. Jacco C. M. Farla et al [8] studied one possible way of decreasing CO_2 emissions, which is to apply CO_2 removal involving recovering of carbon dioxide from energy conversion processes and storing it outside the atmosphere. Since the 1980's, the possibilities for recovering CO_2 from thermal power plants have received increasing attention.

Andrzej Ziebik et al [9] studied the energy analysis of a blast – furnace system operating with the corex process and CO_2 removal. COREX export gas can be utilized in several ways: as fuel gas in a metallurgical CHP, as auxiliary fuel or hot reducing gas in the blast-furnace process (after CO_2 removal), as a reducing agent in the direct reduction of ore (e.g. MIDREX) or as raw gas for the production of synthesis gas. The injection of COREX gas or blast-furnace gas after the removal of CO_2 into the thermal reserve zone influences the consumption of coke, in this way to reduce the emission of harmful components and CO_2 from the cookery. Also it influences the amount of blast furnace gas and its chemical energy, the amount of electricity generated in the blast-furnace gas pressure recovery turbine, the consumption of blast-furnace gas in the Cowper stoves and the amount of blast-furnace gas feeding the gas system of the ironworks. Comparing to conventional BF iron-making system, direct CO_2 emissions of COREX is higher while the total emission depends on the utilization way of export COREX gases [10]. If the export gases are used for power generation and the credits of CO_2 emission are accounted, the COREX smelting

reduction processes can have advantages over conventional BF iron-making system in CO_2 emissions only when the COREX is joined with high-efficiency generating units where the efficiency is greater than 45% and CO_2 emission factor of the grid is higher than 0.9 kg CO_2/kWh.

On the high temperature region of blast furnace (BF) the final reduction step from the wustite (FeO) phase to iron (Fe) depends on direct reduction with solid carbon, which is considered as one of the main factors for CO_2 evolution in the blast furnace. Thus enhancement of the wustite reducibility before the high temperature region will decrease the coke gasification and so decrease the evolved CO_2.

The Egyptian iron ores of El-Baharia Oasis is the main feedstock for the four blast furnaces of the Egyptian Iron and Steel Co. In the present investigation, comparative reduction behavior of synthesized pure chemical wustite and wustite prepared from Baharia iron ore sinter was studied at 1173-1373 K using $H_2/CO/CO_2/N_2$ gas mixture which is somewhat simulating the composition of the reducing gas in case of natural gas injection with low oxygen enrichment in the blast furnace.

II. EXPERIMENTAL

In the present study, two different types of wüstite samples were used for the experiments. The first one is pure chemical sample that is taken as a reference and the other is made of sinter of Baharia iron ore. The pure wustite samples were prepared by the reduction of pure hematite. A reagent grade (A.R) hematite powder (99.9%) was compacted in a cylinder shape. These compacts were sintered at 1473 k in air for 24 hrs. After that the sintered compacts were crushed and reduced to wüstite using a CO/CO_2 gas mixtured at a ratio of 1/1 with a total flow rate of 1 l/min at 1273 K. Due to the non-stoichiometric character of the wüstite, the reaction was extended, after the initial reduction, for about 6 hrs to assure the homogeneous structure distribution of the cation vacancies and holes on the formed wüstite. Pure wüstite powders were compacted into briquettes of about 1 gm weight, 7 mm diameter, and 5 mm height.

For preparation of the other sample, Baharia iron ore sinter was delivered from the Egyptian Iron and Steel Co. in Helwan. The chemical analysis of this sinter as received from the company is shown in Table I. The sinter samples were crushed and reduced to wüstite using a CO/CO_2 gas mixture at a ratio of 1/1 in a total flow rate of 1 l/min at 1273 K.

TABLE I THE CHEMICAL ANALYSIS OF BAHARIA IRON ORE SITER

Fe	SiO_2	CaO	FeO	MgO	Ba
51%	9.8%	9.92%	15.44%	1.75%	1.01%

The prepared wustite samples were then reduced in thermo-gravimetric apparatus at 1173-1373 K using $H_2/CO/CO_2/N_2$ gas mixture. The reduction assembly and gas flow system used in this study were previously mentioned [11]. The course of reduction was followed up by measuring the weight loss as a function of time under controlled conditions of temperature and gas composition. For each reduction experiment, the furnace was heated up to the required reduction temperature, and then the sample was weighed and placed in a platinum wire basket. The sample was then gradually introduced into the furnace so as to avoid thermal shock cracking and positioned in the middle of the furnace constant hot zone. First, nitrogen at a flow rate of 1 liter/min was introduced. Then after the sample soaking for 10 min. at the reduction temperature, the reducing gas mixture at a flow rate of 1 liter/min was introduced. The weight loss resulted from oxygen removal from the briquettes was recorded with time at intervals. At the end of the experiment, the basket with the reduced briquettes was removed and dropped by releasing its suspension wire from the balance, into a conical flask containing acetone to prevent pyrophority of the reduced sample.

The fired and reduced samples were examined with the aid of reflected light microscope (Meiji CK 3900), scanning electron microscope (JEOL, JSM-5410), X-ray diffraction analysis ((JSX-60P JEOL diffractometer with a copper target) and pore size distribution (Micromeritics Pore Sizer 9320).

III. RESULTS AND DISCUSSION

A. Characterization of Prepared Wüstite Samples

The annealed pure wüstite compacts and those prepared from Baharia sinter were characterized with XRD analysis. Wüstite phase clearly appeared in XRD charts, but in case of sinter samples, it was accompanied by other phases appeared such as Ferrobustamite ($Ca_{0.5}Fe_{0.5}SiO_3$) and Ca_2SiO_4 due to the presence of impurities in the ore. From XRD analysis, the average crystalline size was calculated using the diffractions peaks from Scherer's formula as shown below:

$$D = 0.9\,\lambda / \beta \cos\theta \qquad (3.1.1)$$

Where D is the crystallite size, λ the X-ray wavelength, β the broadening of the diffraction peak, and θ is the diffraction angle [12].

It was found that the crystalline size increases from 85.4 nm for pure wüstite to 92 nm for wustite prepared from sinter. Also it can be observed that the total porosity of annealed pure wüstite is 37.28% but for wüstite prepared from sinter of Baharia iron ore is 34.76%. Fig. 1 shows the relation between incremental pore volume and pore diameter for annealed pure wustite compacts and those prepared from sinter of Baharia iron ore. It can be noticed that the pore size distribution in pure wüstite compacts and those prepared from Baharia iron ore mainly ranged between 1-4 and 0.005-0.03 μm. Pure wustite compacts have higher number of large pores whereas wustite prepared from Baharia iron ore has higher number of small pores.

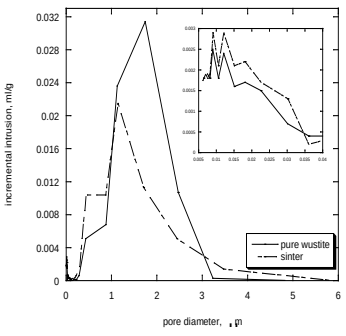

Fig. 1 the pore size distribution for annealed pure wustite and those prepared from sinter of Baharia iron ore.

The microstructure of both wustite samples is a matrix of globular wüstite grains forming a relatively less dense structure with homogeneously distributed macro- and micro-pores. On the other hand, the microstructure of wüstite prepared from sinter showed some changes compared to the pure one as the grains tended to be larger and connected to each other. Also the pores are connected to each other to give larger macropores with denser wüstite grains relative to those in the pure one.

B. Reduction Behavior of Wustite Samples

Using thermo-gravimetric technique, both wüstite samples (pure and those from iron ore sinter) were isothermally reduced at the temperature range 900-1100^{o}C by different ratios of $H_2/CO/CO_2/N_2$ (Table II) which is somewhat simulating the composition of the reducing gas in case of natural gas injection with low oxygen enrichment in the blast furnace. The H_2/CO ratio was in the range of about 0.8-1 that determines the suitable conditions for reduction in the blast furnace to avoid the unfavorable excess of natural gas and CO [13-17]. The reduced samples were characterized by XRD. It was found that the wüstite is reduced gradually to metallic iron. The influence of reduction temperature and reducing gases composition on the reduction behavior and structural characteristics of the reduced products was studied in order to elucidate the kinetics and mechanisms of reduction.

TABLE II THE VARIOUS GAS COMPOSITIONS APPLIED FOR ISOTHERMAL REDUCTION OF WUSTITE SAMPLES

Gas composition, vol%				**$H_2/(H_2+CO+CO_2)$**	**Temp., ^{o}C**
H_2	**CO**	**CO_2**	**N_2**		
15	20	5	60	0.38	900-1100
16.5	18.5	5	60	0.41	
17.5	17.5	5	60	0.44	

1) Effect of Temperature: Pure Samples:

The isothermal reduction curves of pure wüstite compacts reduced by $H_2/(H_2+CO+CO_2)$= 0.38, 0.41 and 0.44 at 900-1100^{o}C are given in Fig. 2-4 respectively. For each single reduction curve, the rate of reduction was highest at the early stages and decreased as reduction proceeds till the end of reduction.

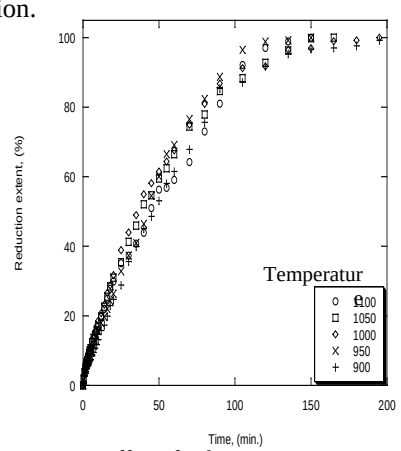

Fig. 2 Effect of reduction temperature on the reduction behavior of pure wustite samples reduced by H_2 / (H_2+CO+CO_2) = 0.38

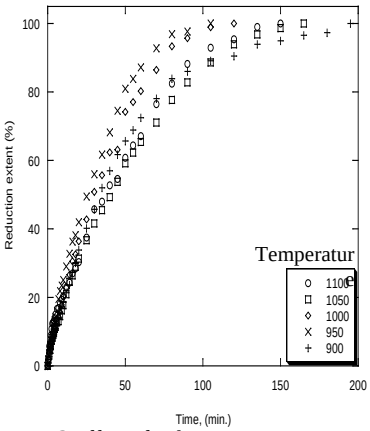

Fig. 3 Effect of reduction temperature on the reduction behavior of pure wustite samples reduced by H_2 / (H_2+CO+CO_2) = 0.41

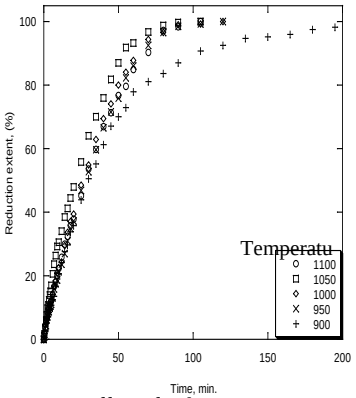

Fig. 4 Effect of reduction temperature on the reduction behavior of pure wustite samples reduced by H_2 / (H_2+CO+CO_2) = 0.44

The reduction came to its completion for all samples reduced by all gas compositions at 900- 1100^{o}C. The effect of temperature on the rate of reduction has a characterized behavior that at the initial stages the reaction rate increased with increasing temperature but gradually becomes independent on reduction temperature. Namely, for $H_2/(H_2+CO+CO_2)$= 0.38 the rate decreased by increasing reduction temperature from 950^{o}C till 1100^{o}C but at 900^{o}C reaction has the lowest rate in this ratio. This phenomenon is due to the possibility of water-gas shift reaction

$$H_2 + CO_2 = CO + H_2O$$

The equilibrium of this reaction is at 800^{o}C, at higher temperatures the reaction shifted to direction of CO formation, which increases percent of CO higher than H_2 in the medium. Since CO has reducing power lower than H_2, so the reduction rate decreased by increasing reduction temperature. Also, for pure wustite compacts reduced by $H_2/(H_2+CO+CO_2)$= 0.41 and 0.44, the reduction rates are independent of temperature due to water-gas shift reaction.

The total reduction process in the blast furnace lasts for 120 min, but the reduction status at 90 min attracts more attention because it is the time needed for the burden to pass through the temperature region of 900-1100^{o}C in a blast furnace. From isothermal reduction curves of pure wustite, it was found that at 900-1100^{o}C the reduction extent after 90 min was in the range of 81-99.5% which is greater than that of pure wustite samples 50-75% isothermally reduced coke gases ($CO/CO_2/N_2$) that studied by the present authors previously [18].

At lower H_2 content, the total porosity decreases by increasing reduction temperature from 53.06% to 28.22% for pure wustite compacts reduced by $H_2/(H_2+CO+CO_2)$= 0.38 at 950^{o}C to 1050^{o}C respectively. The relation between incremental pore volume and pore diameter for pure wustite compacts reduced by $H_2/ (H_2+CO+CO_2)$ = 0.38 at 950 and 1050^{o}C respectively showed that the pore size distribution ranged between 1-10 μm and micropores ranged between 0.007-0.035 μm for both samples. The incremental intrusion value for samples reduced at 950^{o}C is higher than that reduced at 1050 ^{o}C which reflects increasing of pores size and pores number by decreasing reduction temperature which is also confirmed by SEM micrographs as shown in Fig. 5 a, b for pure wustite samples reduced by $(H_2+CO+CO_2)$ = 0.38 at 950 and 1050^{o}C respectively.

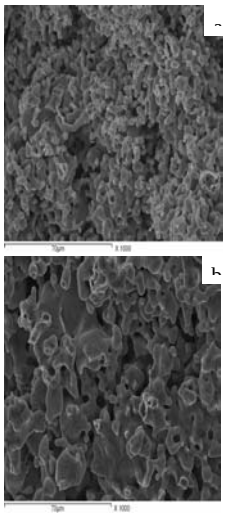

Fig. 5 SEM micrographs of pure wustite reduced by $H_2 / (H_2+CO+CO_2)$ = 0.38

It can be observed that the structure of samples reduced at 950^{o}C contains small grains with some macro- and micro-pores but by increasing temperature, the grains tended to be larger and connected to each other forming dense structure with lower porosity. Accordingly, the faster reduction rate at 950^{o}C increased the porosity of the formed metallic iron compared with reduction at 1050^{o}C.

At higher H_2 percents, total porosity increases by increasing reduction temperature from 33.1% to 56.88% for pure wustite compacts reduced by $H_2/(H_2+CO+CO_2)$= 0.44 at 950^{o}C to 1050^{o}C respectively. The pore size distribution ranged between 1-10μm and micropores ranged between 0.005-0.08 μm for both samples as shown in Fig.6 of pure wustite compacts reduced by $H_2/(H_2+CO+CO_2)$= 0.44 at 950^{o}C to 1050^{o}C respectively. The incremental intrusion value for samples reduced at 1050^{o}C is higher than that for 950^{o}C which reflects increasing of pores size and pores number by increasing reduction temperature as confirmed by SEM micrographs for pure wustite samples reduced by $(H_2+CO+CO_2)$ = 0.44 at 950 and 1050^{o}C.

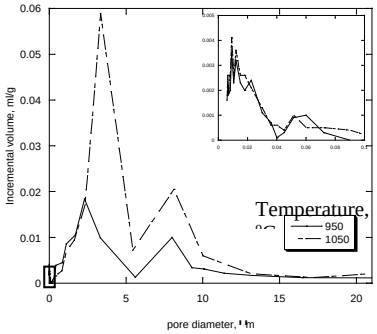

Fig. 6 The relation between incremental intrusion volume and pore diameter for pure wustite reduced by $H_2 / (H_2+CO+CO_2)$ = 0.44 at 950 and

The structure of samples reduced at 950^{o}C is fine and grains agglomerated with each other. But by increasing temperature the grains tended to be larger and connected to each other with many macro- and micro-pores inside them. Accordingly, the faster reduction rate at 1050^{o}C increased the porosity of the formed metallic iron compared with reduction at 950^{o}C.

2) Samples from iron ore sinter:

The rate of reduction was highest at the early stages and decreased as reduction proceeds till the end of reduction. The reduction rate at the early stages increased by increasing the reaction temperature but after that the reduction rate becomes independent on temperature. This is owing to the phenomenon of water-gas shift reaction. On the other hand from isothermal reduction curves, it was found that the reduction extent after 90 min was in the range of 54 - 69% which is relatively higher compared with the wustite from iron ore sinter reduced with coke gases (30 - 50%) as given by industrial data or (34 – 48%) from previous study for present authors [18].

The isothermal reduction curves of wüstite from iron ore sinter reduced by $H_2/(H_2+CO+CO_2)$= 0.41 at 900-1100^{o}C are given in Fig. 7.

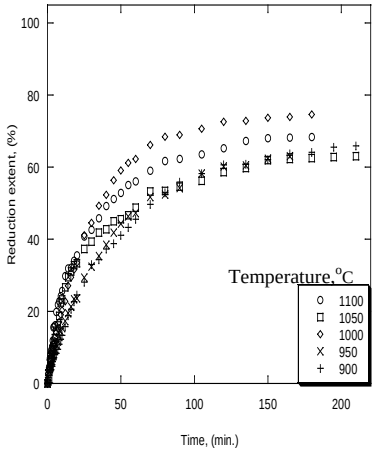

Fig. 7 Effect of reduction temperature on the reduction behavior of iron ore sinter samples reduced by $H_2 / (H_2+CO+CO_2)$ = 0.41

The total porosity increases by increasing reduction temperature from 74.10% to 95.37% for iron ore sinter reduced by $H_2/(H_2+CO+CO_2)$= 0.41 at 900°C to 1100°C respectively. Fig.8 a, b shows the relation between incremental pore volume and pore diameter for wustite from iron ore sinter reduced by $H_2/ (H_2+CO+CO_2)$ = 0.41 at 900 and 1100°C respectively.

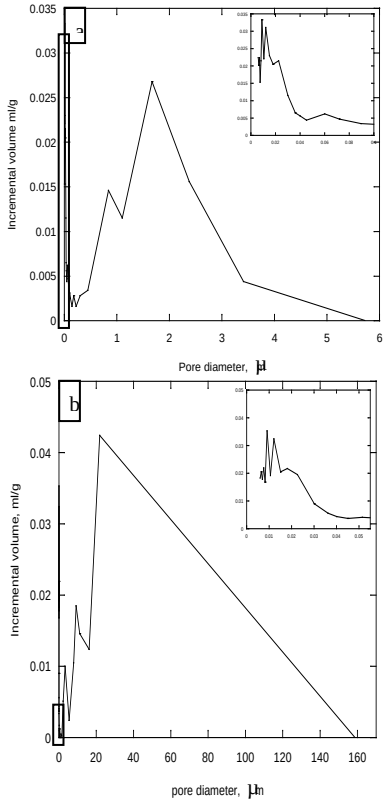

Fig. 8 The relation between incremental intrusion volume and pore diameter for iron ore sinter reduced by $H_2 / (H_2+CO+CO_2)$ = 0.41 at:
a) 900 °C b) 1100 °C

It can be noticed that, for samples reduced at 900°C, the pore size distribution ranged between 0.5-5.5 µm and micropores ranged between 0.01-0.08 µm. But for samples reduced at 1100°C, the pore size distribution ranged between 5-158 µm and micropores ranged between 0.02-0.06 µm. The incremental intrusion value for samples reduced at 1100°C is higher than that at 900°C, and they have a very wide range of macro-pores that reflects increasing of pores' size and pores' number by increasing reduction temperature.

This is confirmed by SEM micrographs as shown in Fig.9 a, b for iron ore sinter reduced by $H_2/ (H_2+CO+CO_2)$ = 0.41 at 900 and 1100°C respectively. It can be observed that the structure of the samples reduced at 1100°C contains whiskers with many micro-pores, and large number of macro-pores but by decreasing temperature the whiskers disappeared and grains tended to be smaller with lower number of macro-pores forming more dense structure.

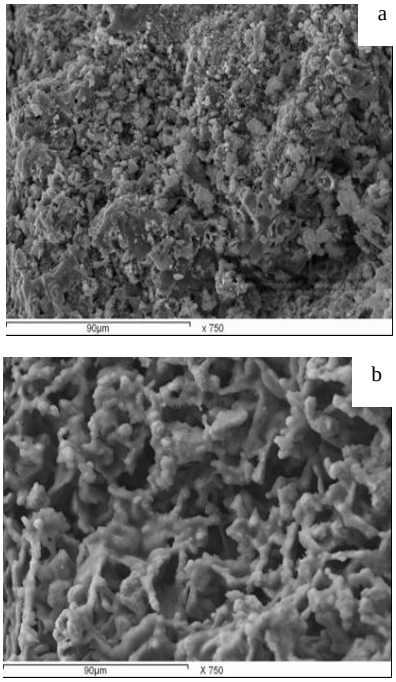

Fig. 9 SEM micrographs of iron ore sinter reduced by
$H_2 / (H_2+CO+CO_2)$ = 0.41 at:
a) 900°C b) 1100°C

3) Effect of Reducing Gas Composition:

Generally it was found that the percent of H_2 in the reducing gases had a significant effect on the reduction of wüstite. The reduction rate increased by increasing H_2 concentration in the reducing gas mix either at high or low temperatures. The difference between reduction rates of various reduced samples decreased by decreasing reduction temperature till 900°C at which the curves overlapped at final reduction stages.

The isothermal reduction curves of pure wüstite compacts reduced by $H_2/ (H_2+CO+CO_2)$ = 0.38, 0.41 and 0.44 at 900 and 1100°C are given in Fig. 10 (a, b) respectively.

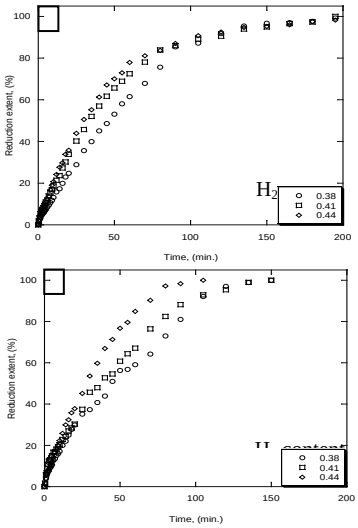

Fig. 10 Effect of reducing gases ratio on the reduction behavior of pure website at:

The internal structures of different pure samples reduced by H_2/ (H_2+CO+CO_2) = 0.38, 0.41 and 0.44 at constant temperatures are examined by SEM. It can be noticed that at higher reaction temperature (1050°C) the produced metallic structure relatively becomes denser by decreasing the H_2 concentration from 0.44 to 0.38. This is also confirmed by the measured total porosity for reduced products at higher temperature, which decreases from 56.88% to 28.22% by decreasing percent of H_2 gas from 44% to 38% respectively. This can be attributed to the relatively slower reaction rate at lower H_2 concentration. Fig. 11 shows the relation between incremental pore volume and pore diameter for pure wustite compacts reduced by H_2/ (H_2+CO+CO_2) = 0.38, 0.41 and 0.44 at 1050 °C.

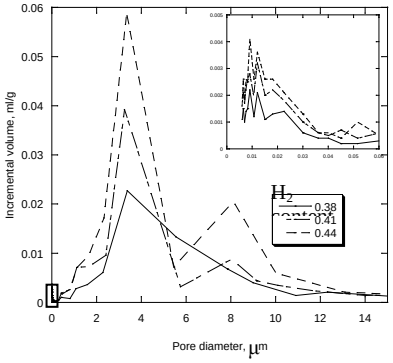

Fig. 11 The relation between incremental intrusion volume and pore diameter for pure wustite reduced by H_2 / (H_2+CO+CO_2) = 0.38, 0.41 and 0.44 at 1050 °C

It can be noticed that the pore size distribution mainly ranged between 1-10 μm and micro-pores ranged between 0.005-0.035 μm for all samples. The incremental intrusion value for sample reduced with H_2 gas percent 0.44 is higher than the others and it has greater number of macro- and micro-pores. This means that pores number increased by increasing H_2 gas percent in reducing gas.

On the other hand, the total porosity for reduced product at lower temperature decreases from 53.06% to 33.1% by increasing percent of H_2 gas from 38% to 44% respectively. Fig.12 shows the relation between incremental pore volume and pore diameter for pure wustite compacts reduced by H_2/ (H_2+CO+CO_2) = 0.38, 0.41 and 0.44 at 950 °C.

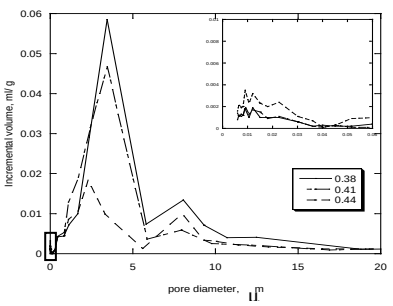

Fig. 12 The relation between incremental intrusion volume and pore diameter for pure wustite reduced by H_2 / (H_2+CO+CO_2) = 0.38, 0.41 and 0.44 at 950 °C

It can be noticed that the pore size distribution mainly ranged between 1-11 μm and micropores ranged between 0.005-0.038 μm for all samples. For macro-pores, the incremental intrusion values increased by decreasing percent of H_2 in reducing gas composition which reflects that the samples reduced by lower H_2 percents have higher number of macro-pores. On the other hand, for micro-pores the incremental intrusion value increased by increasing H_2 percents that confirms increasing rate of reduction by increasing H_2 percent of reducing gas from 0.38 to 0.44 because micropores are mainly responsible for reduction progress.

This also confirmed by studying the internal structure of compacts reduced by H_2/ (H_2+CO+CO_2) = 0.41 and 0.44 at 950°C which showed that micropores increased by increasing percent of H_2 in reducing gas and larger metallic iron areas were formed with lower hydrogen concentration.

4) Samples from iron ore sinter:

The isothermal reduction curves of wüstite samples from iron ore sinter reduced by H_2/ (H_2+CO+CO_2) = 0.38, 0.41 and 0.44 at 1000°C are given in Fig.13. Generally, it is clear that the reduction rate is independent of gas ratio which is due to water gas shift reaction:

$$H_2 + CO_2 = CO + H_2O$$

By increasing percent of H_2 in reducing gas the water gas shift reaction shifted to direction of CO formation so the rate of reduction decreased due to the lower reduction strength of CO compared to that of H_2. However, the reaction was not complete at all reaction conditions.

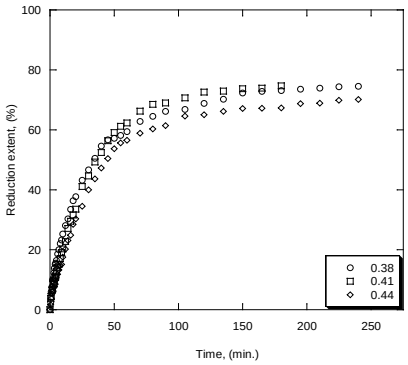

Fig. 13 Effect of reducing gases ratio on the reduction behavior of iron ore sinter at 1000°C

The internal structure of different samples reduced by H_2/ (H_2+CO+CO_2) = 0.38 and 0.44 at constant temperatures (1000°C) are examined by SEM as shown in Fig. 14 a, b respectively.

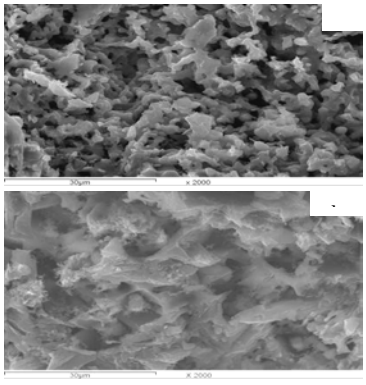

Fig. 14 SEM micrographs of iron ore sinter reduced at 1000 °C by

It can be noticed that the produced metallic iron had a dense structure at higher H_2 concentration while at lower H_2 concentration porous structure was formed. The porosity measurement confirmed the above observations that the total porosity decreased from 87.86% to 67.18 % by increasing reducing gas ratio from 0.38 to 0.44.

The relation between incremental pore volume and pore diameter for wustite from iron ore sinter reduced by $H_2/(H_2+CO+CO_2)$ = 0.38, 0.41 and 0.44 at 1000^{o}C showed that the pore size distribution mainly ranged between 0.4-2.5 μm . For samples reduced by $H_2/(H_2+CO+CO_2)$ = 0.38, but for gas ratio = 0.44 the pore size distribution is slightly wider to 3 μm whereas it mainly ranged between 0.4-5.8 μm. For samples reduced by $H_2/(H_2+CO+CO_2)$ = 0.41 that reflected the presence of a great number of pores with various diameters. The micro pores ranged between 0.005-0.045 μm for all samples. The incremental intrusion values reflected that relatively by increasing H_2 concentration in the reducing gas, number of macro-pores and micro-pores decreased.

B. Rate Controlling Steps and Mechanisms of Reduction

In order to predict the rate controlling mechanism at both the initial and final stages of reduction, the values of apparent activation energy (E_a) are calculated from Arrhenius equation eq. (3.3.1):

$$K_r = K_o\, e^{-Ea/RT} \qquad (3.3.1)$$

Where K_r is the reduction rate constant, K_o is the frequency factor, R is the gas constant and T is the absolute temperature. The application of different heterogeneous gas-solid mathematical models and the internal structure of partially reduced compacts were examined and correlated with each other.

The relationships between the logarithm of the rate of reduction (dr/dt) and the reciprocal of the absolute temperature 1/T are plotted at both initial (20%) and final (80%) reaction stages for pure wüstite samples reduced by $H_2/(H_2+CO+CO_2)$ = 0.44 at 900-1100^{o}C.

From the obtained results, the apparent activation energy (E_a) is calculated at the initial and final stages as shown in Table III**:**

TABLE III THE APPARENT ACTIVATION ENERGY (EA) CALCULATED AT THE INITIAL AND FINAL REDUCTION STAGES FOR PURE WUSTITE SAMPLES REDUCED BY DIFFERENT RATIO OF REDUCING GAS

Reaction stage / **% of Reducing gas**	**Ea values at different ratios of $H_2/(H_2+CO+CO_2)$, (kJ/ mole)**		
	= 0.38	= 0.41	= 0.44
Initial	30.57	37.67	34.12
Final	66.87	57.32	60.3

The values of activation energy indicate the type of mechanism [19]. The calculated activation energy values indicate that the reduction at the initial stages for pure wüstite reduced by $H_2/(H_2+CO+CO_2)$ = 0.38, 0.41 and 0.44 are most likely controlled by combined effect of both gaseous diffusion and interfacial chemical reaction mechanisms while at the final reduction stages it is most likely controlled by interfacial chemical reaction mechanism.

In order to confirm the validity of the reduction mechanism, the following mathematical formulations eq. (3.3.2-3.3.4) derived by Szekely et al. [20-23] was tested against the experimental results:

$$(1)\ t^*(P_F(X)) = X + (1-X)\ln(1-X) \qquad (3.3.2)$$

For gaseous diffusion mechanism

$$(2)\ t^*(G_F(X)) = 1 - (1-X)^{0.5} \qquad (3.3.3)$$

For chemical reaction mechanism

$$(3)\ t^*\left(1 + 1/\sigma^2\right) = G_F(X) + P_F(X)$$

$$= 1 - (1-X)^{0.5} + X + (1-X)\ln(1-X) \qquad (3.3.4)$$

For the mixed control mechanism

where X = fractional reduction degree,

t^* = dimensionless time,

σ = gas-solid reaction modulus.

By applying the different mathematical formulations derived from gas-solid reaction model, it was found that straight lines were obtained on applying the mixed control of the chemical reaction and gaseous diffusion mechanism at the initial reaction stages of pure wustite samples reduced by $H_2/(H_2+CO+CO_2)$ = 0.38, 0.41 and 0.44. Also the straight lines were obtained on applying the chemical reaction mechanism at the final reaction stages of all samples. Fig.15 a, b show the mathematical formulations plots for pure wustite samples reduced by $H_2/(H_2+CO+CO_2)$ = 0.41 at initial and final reduction stages respectively.

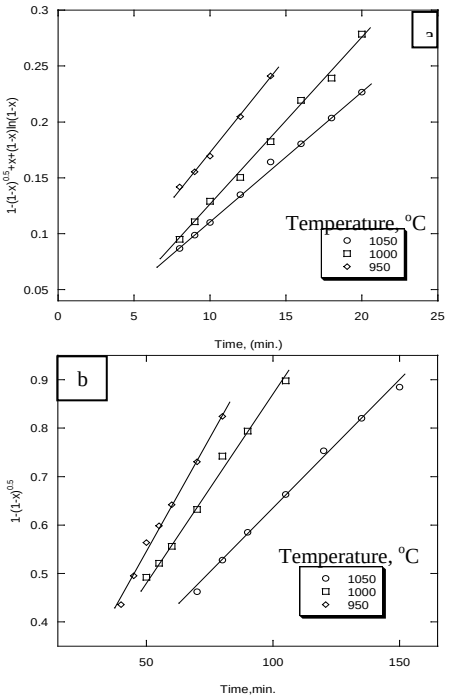

Fig. 15 Application of the control mathematical equation for pure wustite reduced by $H_2/(H_2+CO+CO_2)$= 0.41 at various reduction stages:
a) initial b) final

This was in good agreement with the suggested controlling mechanisms from the calculated activation energy values at both initial and final reduction stages for all samples.

The microstructure of pure wüstite compacts partially reduced by H_2/ (H_2+CO+CO_2) = 0.44 to 20% reduction extent at 1000^{o}C was examined by reflected light microscope as shown in Fig.16a.

It was observed that some micro and macro-pores were observed in homogeneous distribution with the produced metallic iron and wustite grains that reflected the ability of gas access and successful iron nucleation in these samples. At the same time, dense structure of connected wustite grains was detected. So, both gaseous diffusion and interfacial chemical reaction mechanisms are controlling the reaction as concluded above by Ea calculations.

The microstructure of pure wüstite compacts partially reduced by H_2/ (H_2+CO+CO_2) = 0.44 to 80% reduction extent at 1000^{o}C was examined by reflected light microscope as shown in Fig.16b. It was observed that the formed metallic iron structure looks very porous with the presence of many micro and macro-pores in homogeneous distribution for all samples. These observations confirm the concluded reaction controlling mechanisms by Ea calculations.

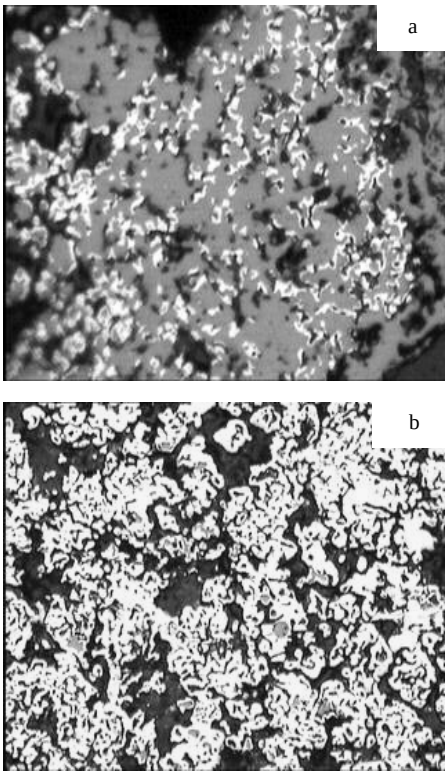

Fig. 16 Photomicrograph of pure wustite samples partially reduced to various reduction extent at 1000 ^{o}C by H_2 / (H_2+CO+CO_2) = 0.44:
a) 20% (x=400) b) 80% (x=200)

The apparent activation energy (E_a) is calculated from the relationships between the logarithm of the rate of reduction (dr/dt) and the reciprocal of the absolute temperature 1/T at both initial (20%) and final (60%) reaction stages for wüstite from iron ore sinter reduced by H_2/ (H_2+CO+CO_2) = 0.41 as shown in the following table:

TABLE IV: THE APPARENT ACTIVATION ENERGY (EA) CALCULATED AT INITIAL AND FINAL REDUCTION STAGES FOR WÜSTITE FROM IRON ORE SINTER REDUCED BY H2/ (H2+CO+CO2) = 0.41

Reaction stage	Initial	Final
Ea values, (kJ/ mole)	35.03	59.06

The values of activation energy indicate the type of mechanism. The reduction at the initial stages for wüstite from iron ore sinter reduced by H_2/ (H_2+CO+CO_2) = 0.41 is most likely controlled by combined effect of both gas diffusion and interfacial chemical reaction mechanisms while at final stages is most likely controlled by interfacial chemical reaction mechanism.

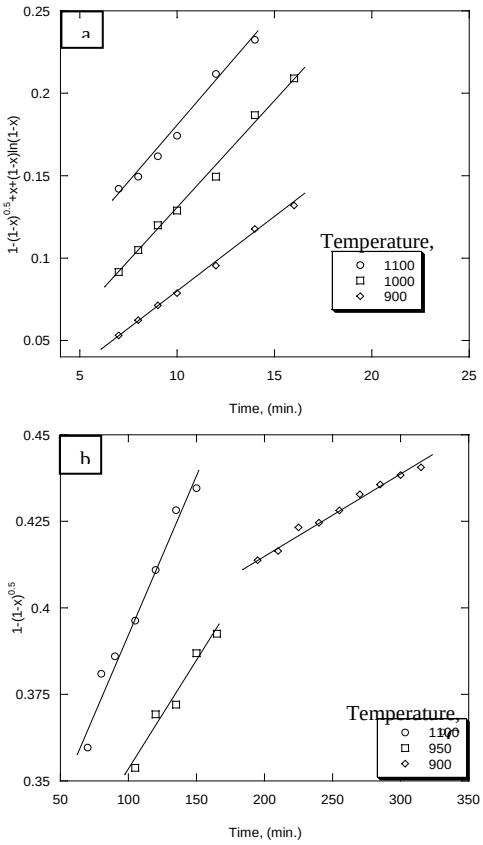

Fig. 17 Application of the control mathematical equation of wustite from iron ore sinter reduced by H_2/ (H_2+CO+CO_2) = 0.41 at:

By applying the different mathematical formulations derived from gas-solid reaction model, it was found that straight lines were obtained on that applying the mixed control mechanism at the initial reaction stages of wustite samples reduced by H_2/ (H_2+CO+CO_2) = 0.41, and at final stages straight lines were obtained on that applying the chemical reaction mechanism as shown in Fig.17a, b respectively. This was in good agreement with the controlling mechanisms suggested from the calculated activation energy values at both the initial and final reduction stages.

The microstructure of wustite from iron ore sinter partially reduced by H_2/ (H_2+CO+CO_2) = 0.41 to 20% and 60% at

1000^{o}C was examined by reflected light microscope. At initial reduction stages, some micro and macropores were in homogeneous distribution with the produced metallic iron and wustite grains that reflected the ability of gas access and successful iron nucleation in these samples. While at final reduction stages metallic iron grains were formed with the presence of many micro and macropores in homogenous distribution forming porous structure, which reflected the easier gas access in this sample.

The concluded mechanism (interfacial chemical reaction) explained the SEM observation in Fig.9b for whisker formation. During the metallic iron formation under pure chemical control, iron is fed to the nucleus down a very steep gradient, which substantiates the extreme assumption that the rate of the transport mechanism is much higher than that of further reduction. Growth then takes place without any significant removal of oxygen around the nucleus a condition which leaves it no other possibility than to grow outwards [24].

IV. CONCLUSIONS

Wüstite samples (pure and those from iron ore sinter) were isothermally reduced at 900-1100^{o}C by different ratios of $H_2/CO/CO_2/N_2$.

The reduction rates of both wustite samples are independent on neither the reaction temperature nor the H2 concentration in the reducing gas mixture due to the water gas shift reaction.

The reduction extent after 90 min. for pure wustite samples is clearly enhanced to be in the range of 81 - 99.5% comparatively with that reduced with coke gases CO/CO2/N2 (50 – 75%).

By the same manner, the reduction extent after 90 min for wustite from iron ore sinter is clearly enhanced to be in the range of 54 - 69% comparatively with that reduced with coke gases (30 - 50%) as industrial data or (34 - 48%) from previous study for present authors.

During reduction of pure wustite, at lower H2 percents the total porosity decreased by increasing reduction temperature while at higher H2 percents, the total porosity increased by increasing reduction temperature.

During reduction of wustite from iron ore sinter, the total porosity increased by increasing reduction temperature.

During reduction of pure wustite, at higher reaction temperature, the produced metallic structure relatively becomes denser by decreasing the H2 concentration while at lower temperature, porosity decreased by increasing percent of H2 gas.

During reduction of wustite from iron ore sinter, the produced metallic iron had a dense structure at higher H2 concentration while at lower H2 concentration porous structure was formed.

The reduction process of pure samples and wüstite from iron ore sinter at initial stages is most likely controlled by the combined effect of chemical reaction and gaseous diffusion mechanisms while at final stages is most likely controlled by interfacial chemical reaction mechanism.

ACKNOWLEDGMENT

This work is fully supported by the Science and Technology Development Fund (STDF), Egypt and is gratefully acknowledged.

REFERENCES

[1] International Panel on Climate Change, *The physical science basis. IPCC*, Geneva, Switzerland, 2007.

[2] Andreas orth, Nikola Anastasijevic and Heinz Eichberger, *Mineral Engineering*, vol. 20, pp. 854-861, 2007.

[3] Zhijia Huang, Xiao Ding, Hao Sun and Siyue Liu, *Journal of cleaner production*,vol. 18, pp. 1052–1058, 2010.

[4] Christer Ryman and Mikael Larsson, *ISIJ International*, vol. 46, No. 12, pp. 1752–1758, 2006.

[5] (2009) http://www.azom.com/news.asp?NewsID=19872, posted Nov 30.

[6] (2009) http://www.gasworld.com/news.php?a=4137.

[7] R. Petela, W. Hutny and J.T. Price, *Advances in Environmental Research*, vol. 6, pp. 157–170, 2002.

[8] Jacco C. M. Farla, Chris A. Hendriks and Kornelis Blok, *Energy Conversion and Management*, vol. 36, Issues 6-9, pp. 827-830, 1995.

[9] Andrzej Ziebik, Krzysztof Lampert and Marcin Szega, *Energy*, vol. 33, pp. 199–205, 2008.

[10] HU Changqing, HAN Xiaowei, LI Zhihong and ZHANG Chunxia, *Journal of Environmental Sciences Supplement*, pp. S116–S120, 2009.

[11] A. A. El-Geassy, M. I. Nasr and M. Bahgat, *Ironmaking Steelmaking*, vol. 27, pp. 117, 2000.

[12] B. D. Cullity and S. R. Stock, *Elements of X-Ray Diffraction*, 3rd edition, pp. 167, Prentice Hall, 2001.

[13] V.N. Andronov, *Modern Blast Furnace*, Library of Saint Petersburg State Technical University, pp. 100, Russia, 2001.

[14] V.N. Andronov, The influence of Different Factors on the Possible Minimum Coke Consumption in the Blast Furnace, *Library of Saint Petersburg State Technical University*, p. 142, Russia, 2001.

[15] K.S. Abdel Halim, Ph.D. Thesis, Saint Petersburg State Technical University, Russia, 2001.

[16] V.N. Andronov and K.S. Abdel Halim, *Journal of ferrous metals (Cherny Metall)*, No.8, pp.25-30, 2001.

[17] K.S. Abdel Halim, V.N. Andronov and M.I. Nasr, *Ironamking and Steelmaking*, vol. 36, No.1, pp. 12-16, 2009.

[18] M. Bahgat, K. S. Abdel Halim, H. A. El-Kelesh and M. I. Nasr, *mineral processing and extractive metallurgy*, vol. 120 , No. 2, pp. 102, 2011.

[19] M. I. Nasr, A. A. Omar, M. H. Khadr and A. A. El-Geassy, *ISIJ International*, vol. 35, pp. 1043, 1995.

[20] J. Szekely, J. W. Evans and H. Y. Sohn, *Gas-Solid Reaction*, Academic press, N. Y, 1976.

[21] H. Y. Sohn and Szekely, *Chem. Eng. Sci.*, vol. 27, pp. 763, 1972.

[22] B. L. Seth and H. U. Ross, *AIME*, vol. 233, pp. 180, 1965.

[23] W. M. Mc Kewan, *AIME*, vol.218, pp. 2, 1960.

[24] R. Nicolle and A. Rist, *Metallurgical Trensactions B*, vol. 10B, pp. 429, 1979.